Cell

Emilin1 Links TGF-β Maturation to Blood Pressure Homeostasis

Luca Zacchigna,[1,5] Carmine Vecchione,[2,5] Antonella Notte,[2] Michelangelo Cordenonsi,[1] Sirio Dupont,[1] Silvia Maretto,[1] Giuseppe Cifelli,[2] Alessandra Ferrari,[4] Angelo Maffei,[2] Carla Fabbro,[4] Paola Braghetta,[4] Gennaro Marino,[2] Giulio Selvetella,[2] Alessandra Aretini,[2] Claudio Colonnese,[2] Umberto Bettarini,[2] Giovanni Russo,[2] Sandra Soligo,[1] Maddalena Adorno,[1] Paolo Bonaldo,[4] Dino Volpin,[4] Stefano Piccolo,[1,*] Giuseppe Lembo,[2,3,*] and Giorgio M. Bressan[4,*]

[1] Developmental Signaling Laboratory, Department of Histology Microbiology and Medical Biotechnologies, University of Padua, viale Colombo 3, 35121 Padua, Italy

[2] Department of Angiocardioneurology, I.R.C.C.S. Neuromed Institute, Loc. Camerelle, 86077 Pozzilli (IS), Italy

[3] Department of Experimental Medicine and Pathology, La Sapienza University, V.le Regina Elena 324, 00161 Rome, Italy

[4] Mouse Genetics Laboratory, Department of Histology Microbiology and Medical Biotechnologies, University of Padua, viale Colombo 3, 35121 Padua, Italy

[5] These authors contributed equally to this work.

*Contact: piccolo@civ.bio.unipd.it (S.P.); lembo@neuromed.it (G.L.); bressan@civ.bio.unipd.it (G.M.B.)

DOI 10.1016/j.cell.2005.12.035

SUMMARY

TGF-β proteins are main regulators of blood vessel development and maintenance. Here, we report an unprecedented link between TGF-β signaling and arterial hypertension based on the analysis of mice mutant for Emilin1, a cysteine-rich secreted glycoprotein expressed in the vascular tree. *Emilin1* knockout animals display increased blood pressure, increased peripheral vascular resistance, and reduced vessel size. Mechanistically, we found that Emilin1 inhibits TGF-β signaling by binding specifically to the proTGF-β precursor and preventing its maturation by furin convertases in the extracellular space. In support of these findings, genetic inactivation of *Emilin1* causes increased TGF-β signaling in the vascular wall. Strikingly, high blood pressure observed in Emilin1 mutants is rescued to normal levels upon inactivation of a single *TGF-β1* allele. This study highlights the importance of modulation of TGF-β availability in the pathogenesis of hypertension.

INTRODUCTION

Arterial hypertension is a major medical problem worldwide, being a risk factor for kidney, cerebral, and coronary heart diseases and affecting about one third of the adult population (Staessen et al., 2003). Hypertension is a complex trait with both genetic and environmental determinants. Although it has been estimated that approximately 30%–50% of blood pressure variance is due to inherited genes, the molecular basis of this disease remains largely to be defined.

Increase in arterial blood pressure levels is commonly attained by an enhanced cardiac pumping and/or an increased vascular resistance to blood flow. So far, studies on the pathogenesis of hypertension have placed major emphasis on smooth muscle and endothelial cells. In contrast, elastic extracellular matrix (ECM), another major component of blood vessels, has been considered for a long time to play only a passive role in the dynamic vascular changes typical of hypertension. However, the use of transgenic animals has recently changed this view, suggesting a causative link between defects in elastic fiber components and the pathogenesis of hypertension (Faury et al., 2003).

A growth factor of key importance in both development and pathophysiology of blood vessels is transforming growth factor-β (TGF-β) (Agrotis et al., 2005). TGF-βs are synthesized as large precursors (proTGF-β) that are cleaved by proprotein convertases (Beck et al., 2002; Annes et al., 2003). This processing step generates a latent TGF-β complex from which the mature ligand must be further released in order to interact with its receptor. Less established is whether proTGF-β is cleaved intracellularly or extracellularly: While earlier reports suggested an intracellular cleavage, recent genetic evidence showed that the TGF-β convertases are required extracellularly (Beck et al., 2002). Of note, only a minor fraction of the total TGF-β produced by the cells is made available for signaling (Annes et al., 2003), suggesting that the balancing between maturation, sequestration, and presentation of TGF-β represents a major regulatory step to set strength and precise localization of TGF-β activity within tissues. Yet surprisingly little is known on the molecules modulating such TGF-β regulatory events in vivo.

Here we provide a novel link between vascular hypertension and dysregulated TGF-β signaling. Our entry point into this field has been the analysis of *Emilin1* knockout mice. Emilin1 is a secreted glycoprotein associated with

the extracellular matrix of blood vessels (Bressan et al., 1993). Emilin1 deficiency causes systemic arterial hypertension. Remarkably, Emilin1 binds only immature proTGF-β and prevents its maturation by protein convertases, thus unveiling a new tier of regulation essential for TGF-β extracellular availability.

This study highlights the importance of ECM components of the vascular system in the pathogenesis of hypertension through the modulation of local TGF-β availability.

RESULTS

Characterization of the Vascular System of Emilin1 Mutant Mice

Emilin1 is the founding member of the EDEN gene superfamily, coding for secreted proteins whose hallmark is the presence of a cysteine-rich motif defined as EMI domain (Braghetta et al., 2004). *Emilin1*$^{-/-}$ mice develop normally and are morphologically indistinguishable from wild-type littermates (Zanetti et al., 2004). This finding suggests either compensatory effects from other Emilin-related proteins or the presence of more subtle phenotypes in *Emilin1* knockout mice.

Emilin1 is strongly expressed in the mouse cardiovascular system during development (Braghetta et al., 2004) and in the adult (Figure 1A). This observation prompted us to thoroughly investigate cardiovascular structure and function of *Emilin1*$^{-/-}$ animals. Strikingly, systemic blood pressure was significantly increased in Emilin1 null mice compared to wild-type littermates, as measured both noninvasively (systolic blood pressure [SBP]: 120 ± 2 versus 101 ± 1, n = 46 per group, $p < 0.01$) and invasively by radiotelemetry, which allows the characterization also of diastolic blood pressure levels (Figure 1B). Remarkably, even blood pressure of heterozygous animals was partially increased (SBP: 112 ± 2, n = 13, $p < 0.01$), indicating haploinsufficiency of *Emilin1* gene for this phenotype. The high blood pressure of mutant animals was observed at all ages examined (from 2 to 12 months) with high penetrance (100% of animals evaluated). However, the increase of arterial pressure in mutant animals with C57BL/6 and CD1 genetic background was higher than that observed in a mixed 129 × C57BL/6 background (mean blood pressure [MBP] increase: 19.3% ± 3.2% versus 12.6% ± 5.3%).

To test whether the increase of blood pressure was dependent on an enhanced cardiac function, we measured cardiac output in anesthetized Emilin1 mutant mice and their wild-type littermates by a pressure/volume tetrapolar catheter. As shown in Figure 1C, cardiac output was similar in both mouse strains. This latter finding was further substantiated by measurement of a series of echocardiographic and hemodynamic parameters of cardiac structure and function, which did not display any significant difference between *Emilin1*$^{-/-}$ and their wild-type littermates in young animals (Table S1). Therefore, cardiac function did not account for the high blood pressure levels observed in mutant mice. In contrast, vascular resistance was significantly augmented in *Emilin1*$^{-/-}$ animals (Figure 1C), thus suggesting that the hypertensive phenotype could be ascribed to vascular abnormalities.

To test whether the increased vascular resistance was due to abnormal vascular contractility or relaxation, second branch mesenteric arteries were explanted, mounted in a myograph, and stimulated with vasoactive drugs. We found no significant difference in the responses of mutant and control arteries (Figures S1A and S1B), suggesting that the increase of peripheral resistance observed in *Emilin1*$^{-/-}$ mice is unlikely due to an abnormal vascular reactivity.

Stiffening of conductance arteries can be a further cause of hypertension (Izzo and Shykoff, 2001). Consequently, the mechanical properties of large arteries were characterized in Emilin1 null mice to look for any significant vascular abnormality. The deformation to increasing applied pressures was recorded on two different kinds of artery, such as aorta and carotid, mounted on a myograph. The diameter versus pressure plots recorded for common carotid artery and ascending aorta gave extensibility values similar in *Emilin1*-deficient and control mice (Figures 1D and S1C; data not shown). However, this analysis revealed an important difference between the two mouse strains: the significant reduction of diameter of blood vessels excised from *Emilin1*$^{-/-}$ compared to wild-type animals at any applied pressure (Figure 1D). Furthermore, this was confirmed by in vivo analysis of ascending aorta by echocardiography (Figures 1E and S1D), by angiography (Figure S1E), and by histological assessment of the vasculature (Figures S1F and S1G). The imaging analysis further clarified that the branches of the vascular tree were not affected by the lack of Emilin1.

Since small blood vessels are the main determinants of peripheral resistance and blood pressure homeostasis, the analysis of the vessel size was extended to resistance vessels. Strikingly, the diameter of isolated second-branch mesenteric arteries under a defined pressure was clearly reduced in *Emilin1* null mice (Figure 1F; 429 ± 21 μm versus 351 ± 23 μm, n = 5 per group, $p < 0.05$), suggesting that the decrease in vessel diameter was a generalized trait of Emilin1 null mice. Noteworthy, the reduction in vessel diameter could be estimated in the order of 20% in both C57BL/6 and CD1 background but was less pronounced and more variable in mice with a mixed 129 × C57BL/6 genetic background (data not shown), suggesting that this vascular trait could be under the influence of modifier genes. Moreover, we found that the lack of Emilin1 realizes a distinctive architecture of resistance vessels with a global reduction of their dimensions both in lumen and media thickness (Figure 1G). Taken together, our data indicate that Emilin1 deficiency does not affect wiring of the vascular system, cardiac performance, and arterial extensibility. In contrast, lack of Emilin1 leads to generalized reduction of blood vessel diameter, increased peripheral resistance, and systemic arterial hypertension.

Emilin1 Inhibits TGF-β Signaling through the EMI Domain

To gain insights into the mechanisms by which Emilin1 controls vascular cell behavior, we focused on the primary structure of the protein. Emilin1 is a multidomain protein: An N-terminal cysteine-rich EMI domain is followed by a coiled-coil, a short collagenous domain, and a C1q-like repeat at the C terminus (Figure 2A). While it has been shown that the C-terminal domain is involved in the oligomerization of Emilin1 and cell adhesion (Mongiat et al., 2000), surprisingly little is known on the function of the EMI domain.

Growth factors' signaling is regulated by secreted molecules containing cysteine-rich repeats, typically also found in various extracellular matrix components (Piccolo et al., 1999). This notion prompted us to explore the possibility that Emilin1 could also modulate growth factors' activity through its EMI domain. To this end, we took advantage of the *Xenopus* embryo as a model system to study signaling pathways in vivo and as a functional read-out for the biological activity of Emilin1 versus endogenous or ectopic TGF-β ligands. Embryos were injected at the two-cell stage with 2 ng of synthetic *Emilin1* mRNA into the marginal zone and then permitted to develop in order to monitor for the appearance of morphological abnormalities. Despite cleaving normally, gastrulation was delayed in Emilin1-expressing embryos, displaying trunk reduction at the tadpole stage (Figure S2B and data not shown). Molecularly, injected embryos showed downregulation of *MyoD* expression (a marker of paraxial mesoderm), as revealed by in situ hybridization carried out at the neurula stage (Figures 2B–2E). Importantly, this biological effect was contributed by the EMI domain and was recapitulated by the injection of mRNA coding for the sole EMI domain (400 pg; Figure 2D), but not of mRNA coding for an Emilin1 molecule deleted of its EMI domain (2 ng, Emilin1ΔEMI; Figure 2E). Overexpression of EMI domain at higher doses (> 1 ng) caused the inhibition of mesoderm development (Figure S2H) and led either to gastrulation failure or to development of embryos with a severely reduced head and trunk (n = 333, 65%; data not shown). Of note, these effects were similar to those of embryos injected with mRNA coding for antagonists of Nodal, a TGF-β family member, such as Cerberus Short (Piccolo et al., 1999) or for cleavage mutant/dominant negative TGF-β ligands (Eimon and Harland, 2002).

These observations raised the possibility that Emilin1 acts through its EMI domain as an inhibitor of TGF-β activity. To test this hypothesis, we first assayed the effects of expressing Emilin1, Emilin1ΔEMI, and EMI domain on the gene responses triggered by Nodal (Xnr-1) in explanted animal cap cells. As shown in Figures 2F and 2G, the induction of the mesoderm markers *Xbra*, *Eomes,* and *Mixer* triggered by *Xnr-1* mRNA was antagonized by coinjection of *Emilin1* or *EMI domain* mRNA but not by coinjection of *Emilin1ΔEMI* mRNA. Interestingly, Emilin1 was unable to counteract the gene response induced by the lowest biologically active dose of a constitutive-active form of the TGF-β receptor (Figure 2H), suggesting that Emilin1 operates upstream of the interaction of the ligand with its receptor. To assess the effect of Emilin1 on TGF-β ligands other than Nodal, we carried out microinjection experiments with *Emilin1* and *TGF-β3* mRNAs. As detailed in Figures S2N–S2Q, Emilin1 was effective in antagonizing the early and long-term phenotypic effects triggered by TGF-β3 in *Xenopus* embryos.

In principle, the phenotypes induced by EMI-domain/Emilin1 overexpression might be compatible with additional effects on other signaling pathways regulating mesoderm development, such as those activated by BMP, FGF, and Wnt growth factors. To address this specificity issue, we compared by RT-PCR the gene responses caused by injection of *BMP2*, *eFGF,* or *Wnt8* mRNAs in the absence or presence of coinjected *EMI-domain* mRNA. As shown in Figures 2I–2K, EMI-domain was unable to counteract the inducing effects of these cytokines. We conclude from these experiments that Emilin1 is a new specific antagonist of TGF-β ligands.

Emilin1 Inhibits proTGF-β Processing by Furin Convertases

Emilin1 may inhibit TGF-β by any of several mechanisms. First, it might interfere with TGF-β secretion or maturation; second, it could prevent the presentation or the interaction of TGF-β ligands with cognate receptors; third, it could act by sequestering either the immature or mature ligand. To test whether the EMI-domain antagonized TGF-β signaling upstream of TGF-β receptor binding, we carried out radio-receptor binding assays using monolayers of HEK293T cells transfected with HA-tagged type II TGF-β Receptor expression plasmid in the presence or absence of a plasmid coding for a GPI-anchored version of the EMI-domain. ^{125}I-labeled TGF-β1 (20 pM) was added to transfected cells and washed; the bound ligand was crosslinked with DSS and then immunoprecipitated with anti-HA antibody. As shown in Figure 3A, binding of ^{125}I-TGF-β1 was competed by cold TGF-β1, though not by EMI-domain.

To further test whether the EMI-domain could antagonize the activity of mature TGF-β irrespectively of competing with the TGF-β Receptor, we concentrated soluble EMI-domain protein from the supernatant of transfected HEK293T cells and tested it for its ability to inhibit the activation of the PAI-1-luciferase (lux) reporter by TGF-β1 in Mv1Lu mink lung cells. Surprisingly, we found that PAI-1-lux induction by recombinant/fully processed TGF-β1 protein was unaffected even by a 50-fold molar excess of EMI-domain protein (data not shown). Similar results were observed upon overexpression of full-length Emilin1 from a transfected plasmid: As shown in Figure 3B, the induction of the Smad reporter CAGA12-luciferase (CAGA12-lux) by recombinant mature TGF-β1 protein was similar in cells expressing Emilin1 or a control cDNA (Figure 3B, lanes 1 and 2); in stark contrast, however, Emilin1 was very effective in inhibiting induction of CAGA12-lux triggered by a cotransfected TGF-β1 expression plasmid (i.e., encoding for

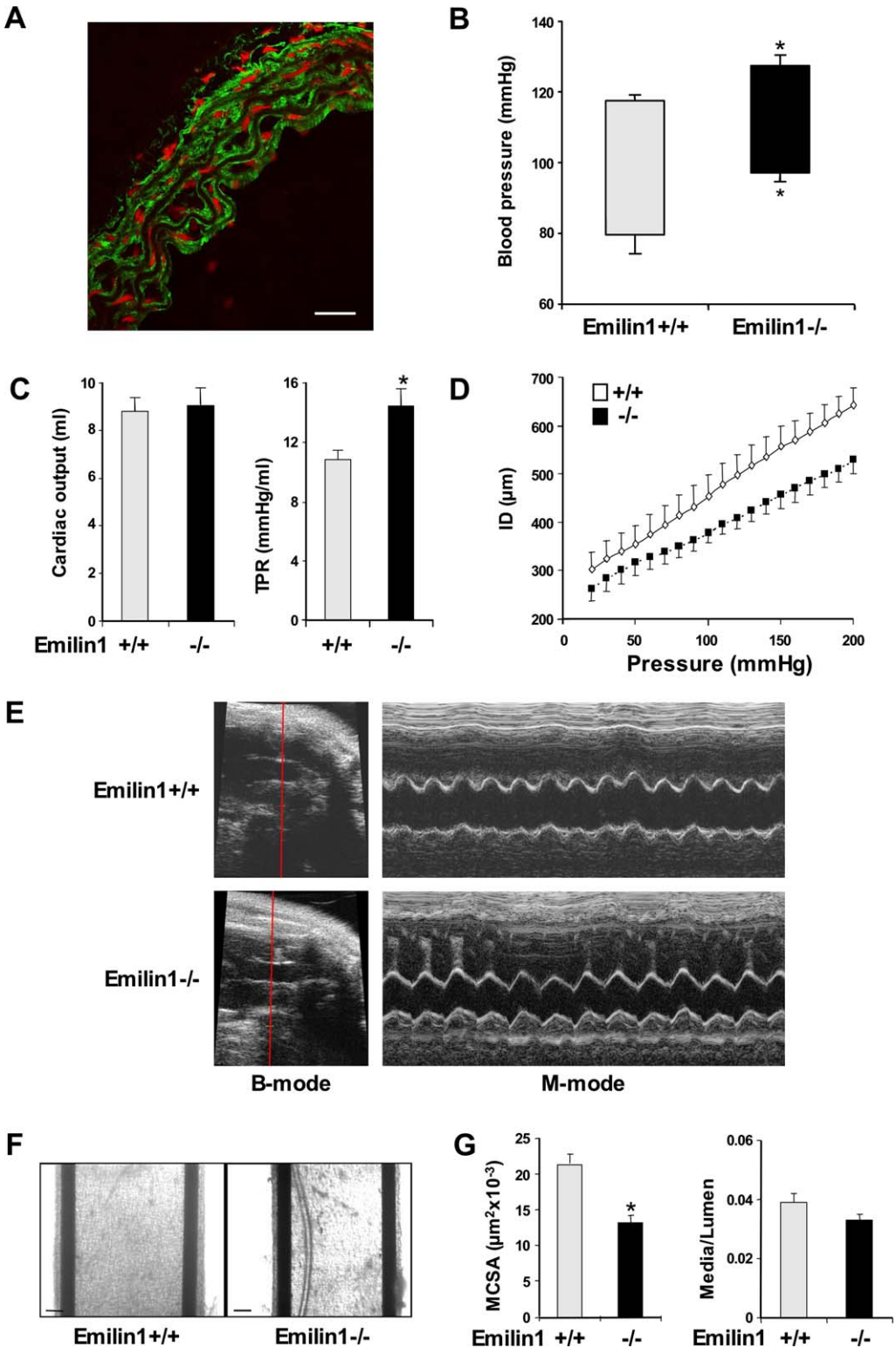

Figure 1. Characterization of the Vascular Phenotype of Emilin1-Deficient Mice

(A) Detection of Emilin1 (green staining) in aorta from adult mouse by immunofluorescence. Nuclei (red) were labeled with propidium iodide solution. Note the preferential location of the protein at the periphery of elastic lamellae. Bar = 25 μm.

biologically active proTGF-β1 C223S/C225S) (Figure 3B, compare lanes 3 and 4). This effect was specific and relied on the EMI-domain, as Emilin1ΔEMI had no effect and transfection of the sole EMI-domain had similar, albeit weaker, activity to that of full-length Emilin1 (Figure 3B, lanes 5 and 6).

To validate these conclusions in more physiological conditions, we compared the response of a natural TGF-β target in normal and *Emilin1* mutant primary mouse embryonic fibroblasts (MEFs). For this purpose, we used the promoter of the CDK-inhibitor $p15^{Ink4b}$ (p15-lux). As shown in Figure 3C, the transcription from p15-lux is higher in *Emilin1* knockout cells when compared to wild-type cells (lanes 1 and 2); remarkably, blockade of TGF-β receptor activity in mutant cells with the drug SB431542 (Inman et al., 2002) reversed this effect (lane 3), indicating that endogenous Emilin1 is required to restrain TGF-β activity in MEFs. If Emilin1 limits endogenous TGF-β signaling, Emilin1 deficiency should parallel with an enhanced responsiveness to autocrine TGF-β synthesis. To test this hypothesis, we treated wild-type and Emilin1 mutant MEFs with a chemical inhibitor of JNK1/2 (SP600125); indeed, it has been recently shown that loss of JNK turns on the transcription from the endogenous TGF-β1 promoter, setting up a sustained production of autocrine TGF-β1 in MEFs (Ventura et al., 2004). As shown in Figure 3D, using p15-lux assays we found that *Emilin1* mutant MEFs display a greater sensitivity than wild-type MEFs to JNK blockade, supporting the notion that lack of Emilin1 causes aberrant TGF-β signaling.

Next, we asked whether the biochemical target of Emilin1 is proTGF-β1, namely, the immature and inactive precursor of TGF-β1. HEK293T cells were transfected with a proTGF-β1 expression construct alone or in combination with a plasmid directing the expression of EMI-domain on the cell surface (Flag- and GPI-tagged) (Figure 3E). Cell lysates were subjected to immunoprecipitation with anti-Flag antibody, and proteins copurifying with the EMI-domain were analyzed by Western blot using an anti-LAP antibody. As shown in Figure 3E, the EMI-domain interacted with proTGF-β1.

We then wished to verify that the EMI-domain interacted specifically with pro-TGF-β1 rather than with the processed small-latent complex (LAP bound to processed TGF-β) or free LAP. To this end, we repeated the pull-down experiments using EMI-domain with extracts containing proTGF-β, LAP protein alone, or a precomplexed LAP/TGF-β1. As shown in Figure 3F, the EMI-domain bound efficiently only to proTGF-β1. This interaction also occurred at physiological levels of Emilin1, as demonstrated by the copurification of endogenous Emilin1 with proTGFβ1 (Figure 3G).

The proteolytic processing of the proTGF-β precursor is an essential step in the formation of the biologically active TGF-β ligand. Since Emilin1 can interact with proTGF-β1, we tested whether its inhibitory activity on TGF-β signaling relied on inhibition of the proteolytic clipping of proTGF-β. HEK293T cells were transfected with plasmids expressing proTGF-β1 alone or in combination with Emilin1 or EMI-domain. As shown in Figure 3H, immunoblot analysis of the cell lysates and conditioned medium from these cultures revealed that both Emilin1 and EMI-domain potently inhibited the cleavage of proTGF-β1 into LAP (~46 kDa band) and TGF-β1 ligand (12 kDa band), while having no effect on total proTGF-β1 synthesis (~50 kDa band). This conclusion was supported by the inhibition of Smad2 phosphorylation in HepG2 cells treated with the conditioned media collected from cells expressing proTGF-β1 in the absence or presence of Emilin1 (Figure S3A).

The effect of Emilin1 is similar to that produced by treatment of cells with RVKR-CMK, a drug blocking the activity of endogenous furins (Figure 3I). Moreover, ectopic expression of the proprotein convertase SPC1 led to the appearance of a smaller 43 kDa band, whose formation was also inhibited by transfected EMI-domain (Figure 3J). To test the relevance of Emilin1 in limiting TGF-β1 processing in vivo, we compared the steady state levels of transfected proTGF-β1 in wild-type and *Emilin1* knockout MEFs. As shown in Figure 3K, lack of Emilin1 caused the disappearance of the 50 kDa proTGF-β1 band (compare lanes 1 and 2); crucially, blockade of furin activity rescued the level of proTGF-β1 in $Emilin1^{-/-}$ MEFs (lane 3). Taken together,

(B) Systolic and diastolic blood pressure evaluated in $Emilin1^{+/+}$ and $Emilin1^{-/-}$ mice invasively by radiotelemetry in conscious mice (n = 3 per group). *p < 0.05 versus wild-type mice. Data are mean ± SEM. Blood pressure continued to be higher in $Emilin1^{-/-}$ mice also during anesthesia (MBP: 116 ± 3 versus 101 ± 2 mmHg, p < 0.01).

(C) Cardiac output and total peripheral resistance (TPR) evaluated in wild-type and *Emilin1* knockout mice by Millar catheter placed in the left ventricle (n = 7 per group). *p < 0.05 versus wild-type mice. Data are mean ± SEM.

(D) Pressure-internal diameter (ID) relationship for common carotid arteries from $Emilin1^{+/+}$ (empty diamonds) and *Emilin1*-deficient (filled squares) mice. The arteries were placed on a Mulvany pressure system and subjected to increasing intraluminal pressure (n = 6 per group). Data are mean ± SEM. Note that mutant vessels, although displaying a smaller diameter compared to wild-type at any applied pressure, do respond normally (similar slope) to pressure increments. Values from mutants were significantly different from wild-type at any pressure (p < 0.05). These data were used to calculate extensibility values as shown in Figure S1C.

(E) Detection of reduced diameter of ascending aorta in Emilin1 deficient mice. Left panels: B-mode (bidimensional mode) echocardiography images to allow the appreciation of landmarks. Right panels: M-mode (mono-dimensional mode) imaging of the section selected as shown in the B-mode image.

(F) Images of mesenteric arteries from control and Emilin1-deficient mice mounted in a Mulvany myograph showing reduction of vessel diameter. (Bar = 50 μm).

(G) Evaluation of media cross-sectional area (MCSA) and media/lumen ratio (M/L) in mesenteric arteries from wild-type and Emilin1 mutant mice (n = 5 for each group). *p < 0.05 versus wild-type mice. Data are mean ± SEM.

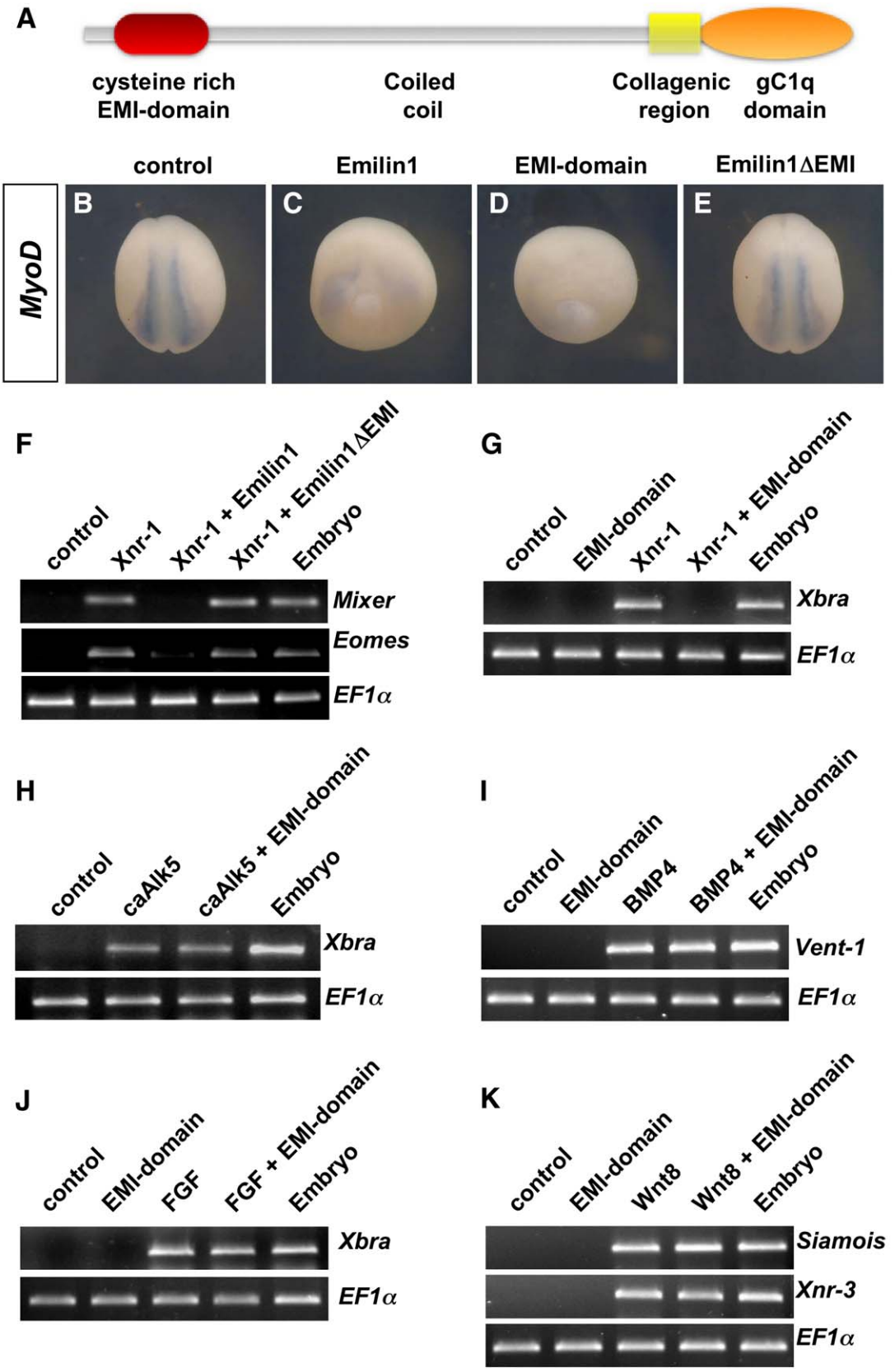
A
cysteine rich EMI-domain
Coiled coil
Collagenic region
gC1q domain
control
Emilin1
EMI-domain
Emilin1ΔEMI
MyoD
B
C
D
E
F
control
Xnr-1
Xnr-1 + Emilin1
Xnr-1 + Emilin1ΔEMI
Embryo
Mixer
Eomes
EF1α
G
control
EMI-domain
Xnr-1
Xnr-1 + EMI-domain
Embryo
Xbra
EF1α
H
control
caAlk5
caAlk5 + EMI-domain
Embryo
Xbra
EF1α
I
control
EMI-domain
BMP4
BMP4 + EMI-domain
Embryo
Vent-1
EF1α
J
control
EMI-domain
FGF
FGF + EMI-domain
Embryo
Xbra
EF1α
K
control
EMI-domain
Wnt8
Wnt8 + EMI-domain
Embryo
Siamois
Xnr-3
EF1α

these findings suggest that Emilin1 (or the isolated EMI-domain) protects proTGF-β from proteolytic activation.

Next, we wished to know whether the inhibition of TGF-β1 by Emilin1 occurs in the intracellular or extracellular space. To address this question, we prepared two populations of HEK293T cells—responding and stimulator cells—and carried out cell-mixing experiments. The responding cells (indicated as R in Figure 3L) contained the TGF-β reporter CAGA12-lux; the stimulator cells (indicated as S in Figure 3L) were the source of TGF-β1. As expected, when stimulator cells were mixed with responding cells, CAGA12-lux was induced (Figure 3L, lanes 1 and 3). To establish where Emilin blocked proTGF-β1, full-length Emilin1 expression plasmid (indicated as +E in Figure 3L) was cotransfected in stimulator or responding cells. Remarkably, the presence of Emilin1 either in the stimulator or responding cells equally inhibited the TGF-β response (Figure 3L, lanes 4 and 5), indicating that Emilin1 can operate non-cell-autonomously in antagonizing proTGF-β signaling. To validate this conclusion at the endogenous level, we carried out cell-mixing experiments using wild-type and *Emilin1* null MEFs (Figure 3M). In this setup, responding cells were transfected with the natural TGF-β reporter p15-lux, and the stimulator cells were induced to increase the endogenous production of TGF-β1 by treatment with JNK inhibitors (Ventura et al., 2004). Combinations of wild-type responding with untreated wild-type or *Emilin1* knockout cells led to comparable basal levels of transcription (Figure 3M, lanes 1 and 2), with higher levels in the combination mutant responding/untreated mutant cells (lane 3), in line with the enhanced TGF-β signaling of mutant cells. As expected, upon induction of endogenous TGF-β synthesis with the JNK inhibitor SP600125, the combination knockout-responding/knockout-stimulator gave stronger activation of p15-lux promoter than the combination wild-type responding/wild-type stimulator (lanes 4 and 5). Intriguingly, when the induced knockout-stimulator cells were mixed with wild-type-responding cells, the level of TGF-β signaling was similar to the full wild-type combination (compare lanes 5 and 6); this suggests that endogenous Emilin1 in the responding cells antagonized proTGF-β extracellularly. This conclusion was finally validated by using a nonsecretable KDEL-tagged Emilin1, a signal that has been shown to cause retention of a secreted protein within the secretory vescicles up to Trans-Golgi space. As shown in Figure 3N, cells transfected with KDEL-Emilin1 actually displayed an enhanced, rather than an inhibited, TGF-β1 responsiveness. Taken together, these gain- and loss-of-function experiments indicate that Emilin1 is relevant to prevent TGF-β processing outside of the cell.

Reversal of the Emilin1 Null Hypertensive Phenotype by Reduction of TGF-β Gene Dosage

Since TGF-β ligands and Emilin1 are coexpressed in vascular smooth muscle cells of the aortic wall, the data presented above suggest that Emilin1 plays a role in restraining TGF-β effects within the vascular tissue. To test the requirement of Emilin1 in the control of TGF-β signaling in vivo, we searched for proof of increased TGF-β signaling in the vascular system of *Emilin1*$^{-/-}$ mice.

As a first indicator of TGF-β signaling, the relative abundance of nuclei staining with antibodies to phospho-Smad2 (P-Smad2) was measured. The number of P-Smad2 positive nuclei were significantly increased in mutant aorta (Figures 4A–4C). The construct CAGA12-GFP, in which the GFP reporter gene is under the control of multimerized TGF-β responsive elements, was used as a second, independent read-out of TGF-β activity. Transgenic mice carrying this construct were crossed with Emilin1 mutant mice, and expression of the GFP reporter gene in aorta was revealed with anti-GFP antibodies on histological sections. The intensity of immunochemical reaction was higher in the mutant than in the wild-type background (Figures 4D and 4E), indicating an increased activation of the CAGA12 promoter in Emilin1-deficient aorta.

Together, our biochemical and functional evidence revealed an intriguing role for Emilin1 in the control of TGF-β activity that may be functionally relevant in the context of blood vessels. If Emilin1 acts within the TGF-β pathway to promote vascular remodeling and hypertension, the reduction of *TGF-β1* gene dosage should attenuate the mutant phenotype. Strikingly, inactivation of one *TGF-β1* allele in *Emilin1* null animals was sufficient to bring blood pressure levels back to normal (Figures 4G and 4I, compare *Emilin1*$^{-/-}$*;TGFβ1*$^{+/+}$ with *Emilin1*$^{-/-}$*;TGFβ1*$^{+/-}$ mice).

Figure 2. Emilin1 Inhibits Nodal/TGF-β Signaling through the EMI Domain

(A) Schematic representation of the structure of Emilin1 protein. The EMI domain at the N terminus is a cysteine-rich region distinctive of the EDEN protein family.

(B–E) Overexpression of Emilin1 attenuates mesoderm development in *Xenopus* embryos through the EMI-domain. Eight cell-stage embryos were injected in the marginal zone with mRNAs encoding for full-length Emilin1 (2 ng) (C), EMI-domain alone (400 pg) (D), or a deleted version of Emilin1 (2 ng, Emilin1ΔEMI) lacking the EMI-domain (E). The embryos were processed by in situ hybridization for the paraxial mesoderm marker *MyoD*. Similar results were obtained by staining gastrula stage embryos with the pan-mesodermal marker *VegT* (Figure S2).

(F and G) Emilin1 inhibits nodal/TGF-β signaling, and this requires the EMI-domain. Two cell-stage embryos were injected in the animal pole with the indicated mRNAs. Animal caps were explanted at stage 9 and harvested at stage 11 for RT-PCR analysis. (F) Activation of the mesoderm markers *Eomes* and *Mixer* by *Xnr-1* mRNA (60 pg) is antagonized by *Emilin1* mRNA but not by *Emilin1ΔEMI* mRNA. (G) Overexpression of *EMI-domain* mRNA is sufficient to inhibit mesoderm induction by coinjected *Xnr-1.* As shown in Figure S2, induction of ectopic bottle cells or axial structures, typical effects of TGF-β/Nodal/Smad signaling, is also antagonized by Emilin1.

(H) RT-PCR of animal caps explanted from embryos injected as in (F) with *constitutive-active (ca)-TGF-β type I receptor (Alk5)* mRNA (100 pg) alone or in combination with *EMI-domain* mRNA (800 pg). Emilin1 acts upstream of TGF-β receptor activity.

(I–K) Embryos were injected as in (F) with *EMI-domain* mRNA (800 pg) in combination with *BMP2, eFGF,* or *Xwnt8* mRNAs (100 pg, 2 pg, and 20 pg, respectively). Explanted animal caps were analyzed by RT-PCR for the indicated markers. *EF1α* serves as loading control.

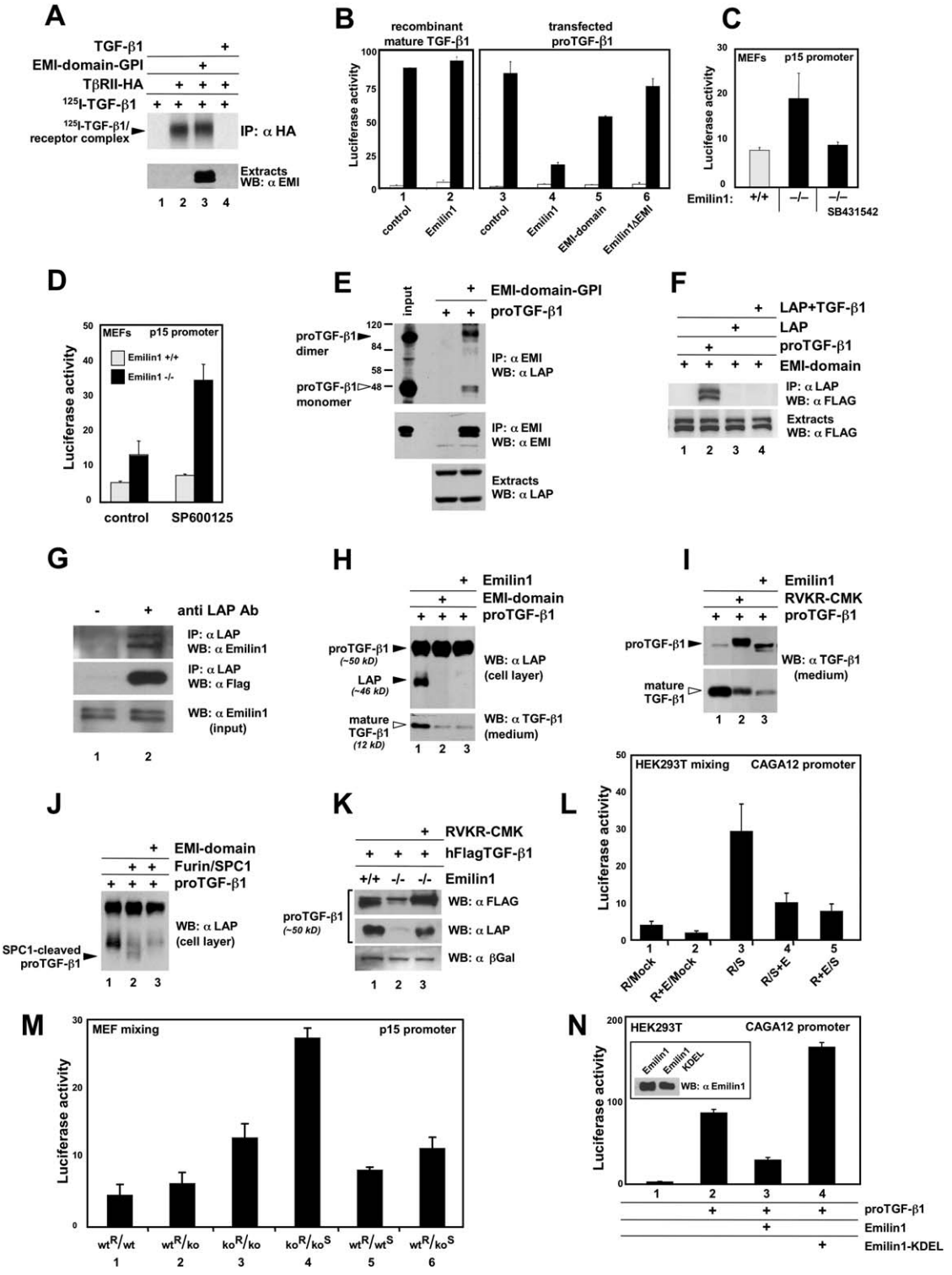

Figure 3. Emilin1 Inhibits Cleavage of the Mature TGF-β1 Ligand from the proTGF-β1 Precursor

(A) EMI-domain does not compete with radiolabeled recombinant TGF-β1 for binding to type II TGF-β receptor. Anti-HA immunoprecipitates were resolved by SDS-PAGE prior to autoradiography. Cold TGF-β1, though not EMI-domain, inhibits complex formation.

(B) Emilin1 inhibition of TGF-β1 signaling depends on its EMI-domain. The CAGA12-lux reporter (100 ng/2 cm well) was transfected in HEK293T cells alone or in combination with Emilin1 expression plasmids (500 ng) as indicated. After transfection, cells were either left untreated (white bars) or treated overnight with 5 ng/ml recombinant TGF-β1 (black bars—lanes 1 and 2). In lanes 3–6, cells were cotransfected with Emilin and proTGF-β1

Moreover, upon reduction of *TGF-β1* gene dosage, the size of *Emilin1*$^{-/-}$ vessels returned normal in both resistance (Figure 4H) and conductance (Figure 4I) districts.

The reduced size of *Emilin1*$^{-/-}$ blood vessels suggested a role for Emilin1 as a positive regulator of cell proliferation. Indeed, TGF-β is well known to deliver a potent cytostatic signal to diverse cell types, including primary smooth muscle cells (SMC) (Siegel and Massague, 2003; Khanna, 2004). To explore this possibility, we isolated primary SMC from aortas of wild-type and Emilin1 mutant 15-day-old mice and measured their growth capacity using an in vitro cell proliferation assay. Mutant SMC showed a significant reduction of proliferation compared with wild-type cells (Figure S4A). These results are consistent with the notion that an enduring activation of the TGF-β cascade from early stages of development to adult life generates a negative bias on growth in vascular cells, as observed in the generalized reduction of blood vessels size in Emilin1-deficient mice. Accordingly, we found a reduced level of c-Myc expression in aortic tissue explanted from Emilin1 mutant mice (Figure S4B). c-Myc is a negatively regulated direct target of TGF-β/Smad signaling, and its repression is pivotal for ligand-mediated activation of $p21^{WAF1}$ and $p15^{INK4b}$ CDK inhibitors (Siegel and Massague, 2003). Remarkably, c-Myc levels returned to normal in aortas taken from the combined *Emilin1* null/*TGF-β*$^{+/-}$ mutants (Figure S4B, lane 3), a finding in line with the rescue of the vascular phenotype (Figure 4G–4I). Taken together, these data support the notion that Emilin1 is a novel inhibitor of TGF-β availability in vivo.

Emilin1 is not the only ECM protein suggested to regulate TGF-β signaling. The case of Fibrillin-1 deserved particular attention, as it has been shown to be a negative regulator of TGF-β. In transgenic mouse models of Marfan syndrome, the increased volume of lung alveoli has been correlated with upregulation of TGF-β reporter CAGA12, the same used here. This lung phenotype can be cured with inactivating antibodies for TGF-β (Neptune et al., 2003). These data raised the possibility that Emilin1 may be influencing TGF-β signaling by a secondary mechanism through Fibrillin-1. We therefore investigated the consequences of Emilin1 deficiency on deposition and maintenance of Fibrillin-1 microfibrils. The pattern of distribution of Fibrillin-1 was indistinguishable in *Emilin1*$^{+/+}$ and *Emilin1*$^{-/-}$ aortas and MEFs (Figures S5A–S5D). These results rule out the presence of major abnormalities of the microfibrillar system in Emilin1 mutants.

Like Fibrillin-1, Emilin1 is expressed at high levels in lung (Braghetta et al., 2004). The Fibrillin-1 paradigm maintains that excess TGF-β should lead to increased alveolar spaces (Neptune et al., 2003). This hypothesis was validated experimentally by histological analysis. As shown in Figures 4J–4L and quantitatively analyzed in Figure 4N, lack of Emilin1 induced a significant increase of alveolar dimensions, as did Fibrillin-1 deficiency. The identification of such TGF-β-dependent phenotype clearly

expression plasmids, encoding for the C223S/C225S mutant that does not require acidic activation (40 ng). Values indicate mean ± sd. Note that Emilin cannot antagonize mature TGF-β1. Accordingly, we found in heterologous frog assays that recombinant, fully processed hActivin was not antagonized by *Emilin1* mRNA expressing cells (data not shown).

(C and D) Primary MEFs were transfected with the TGF-β reporter p15-lux. The higher transcriptional response in *Emilin1*$^{-/-}$ cells is reversed to wild-type levels upon treatment with the TGF-β receptor inhibitor SB431542 (C) and fostered by the JNK inhibitor SP600125 (D). Values are mean ± sd.

(E) Emilin1 interacts with proTGF-β1. HEK293T cells were transfected with the proTGF-β1 and Flag-tagged EMI domain-GPI expression plasmids (8 μg/10 cm diameter dish). Cell lysates were subjected to immunoprecipitation (anti-Flag) and Western blot (anti-LAP). In similar experimental setups, we found that the overexpressed EMI domain can also interact with proActivin-HA, proNodal-HA, and proTGF-β3-HA (data not shown).

(F) The small latent complex does not interact with Emilin1. Immunoprecipitation (anti-Flag antibody) of HEK293T cells transfected with the expression plasmid for Flag-tagged EMI-domain-GPI and supplemented with recombinant LAP or precomplexed LAP/TGF-β or cotransfected with proTGF-β1 expression plasmid. Anti-LAP immunoblotting reveals a specific interaction with proTGF-β.

(G) Overexpressed TGF-β interacts with endogenous Emilin1. HEK293T cells were transfected with proTGF-β alone and processed as in (E) to reveal the copurification of endogenous Emilin1.

(H) Emilin1 inhibits proTGF-β1 processing. HEK293T cells were transfected with the indicated expression plasmids for proTGF-β1 (1 μg/3.5 mm diameter plate), Emilin1 (2 μg), and EMI domain (1 μg). Western blotting of the cell lysates (cell layer) and of the conditioned supernatants (medium) shows that transfected proTGF-β1 is cleaved into LAP and mature TGF-β1 by endogenous convertases' activity (lane 1), which are inhibited in the presence of EMI domain (lane 2) or full-length Emilin1 (lane 3).

(I) Emilin1 phenocopies furin inhibition. HEK293T cells were transfected as in (F). Where indicated, cells were treated with the furin inhibitor RVKR-CMK. The conditioned medium was analyzed by immunoblotting with anti-Flag antibody.

(J) EMI domain inhibits cleavage of proTGF-β1 by overexpressed furin/SPC1. HEK293T cells were transfected with the indicated expression plasmids for proTGF-β1 (1 μg/3.5 mm diameter plate), furin/SPC1 (2 μg), and EMI domain (2 μg). Overexpression of SPC1 enhances cleavage of proTGF-β1 (black arrowhead, lane 2), and this effect is reversed by overexpression of EMI domain (lane 3). This effect is specific, as EMI domain does not interfere with proBMP processing (Figure S3B).

(K) Emilin1 is required to prevent proTGF-β cleavage. Lanes 1 and 2, wild-type and *Emilin1* mutant MEFs expressing transfected proTGF-β; lane 3, inhibition of furins rescues proTGF-β stability in mutant cells but has no effect on wild-type cells (data not shown).

(L and M) Emilin1 inhibits proTGF-β activity in the extracellular space. Cell mixing experiments were carried out as described in the text. Abbreviations are: R, responding cells; Mock, control-untreated cells; S, stimulator cells producing proTGF-β; +E indicates that cells were also transfected with Emilin1 expression plasmid. Note that in lane 5 of (L) Emilin1 is efficient in blocking signaling when expressed in cells not producing proTGF-β. In (M), abbreviations are: wt, wild-type MEFs; wt^R, Responding wild-type MEFs; ko, *Emilin1* knockout MEFs; ko^R, Responding *Emilin1* knockout MEFs; ko^S, Stimulator *Emilin1* knockout MEFs; wt^S, Stimulator wild-type MEFs. Values indicate mean ± sd.

(N) Emilin1 must be secreted to antagonize TGF-β signaling. Overexpression of Emilin-tagged with KDEL is incapable of antagonizing the effect of cotransfected proTGF-β. Inset: Western blot showing comparable expression levels of the transfected proteins. The increased signaling in Emilin-KDEL-expressing cells suggests a dominant negative effect on endogenous Emilins. Values indicate mean ± sd.

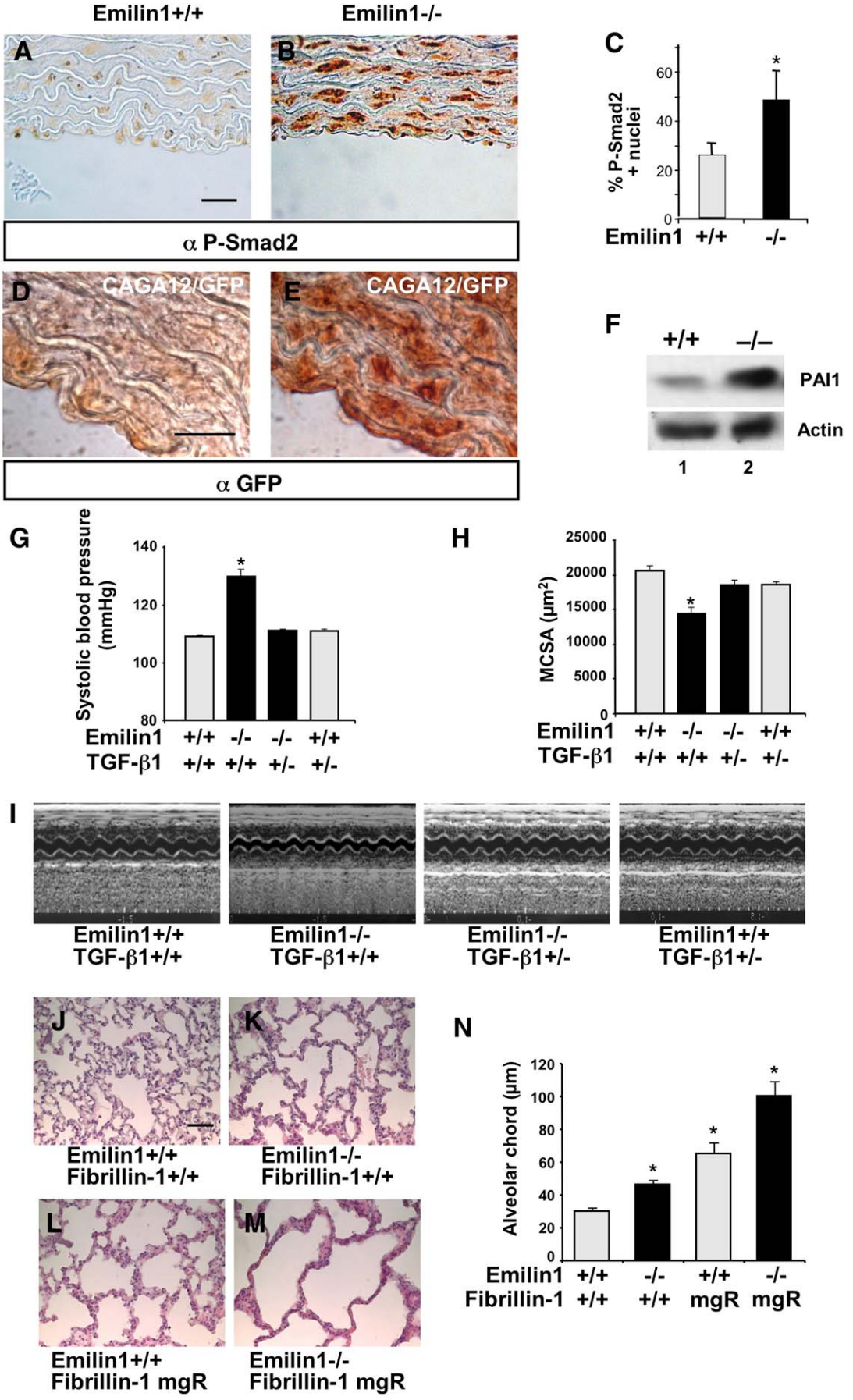
Emilin1+/+
Emilin1-/-
A
B
α P-Smad2
C
% P-Smad2 + nuclei
60
40
20
0
*
Emilin1 +/+ -/-
D
CAGA12/GFP
E
CAGA12/GFP
α GFP
F
+/+ –/–
PAI1
Actin
1 2
G
Systolic blood pressure (mmHg)
140
120
100
80
*
Emilin1 +/+ -/- -/- +/+
TGF-β1 +/+ +/+ +/- +/-
H
MCSA (μm²)
25000
20000
15000
10000
5000
0
*
Emilin1 +/+ -/- -/- +/+
TGF-β1 +/+ +/+ +/- +/-
I
Emilin1+/+ TGF-β1+/+
Emilin1-/- TGF-β1+/+
Emilin1-/- TGF-β1+/-
Emilin1+/+ TGF-β1+/-
J
K
Emilin1+/+ Fibrillin-1+/+
Emilin1-/- Fibrillin-1+/+
L
M
Emilin1+/+ Fibrillin-1 mgR
Emilin1-/- Fibrillin-1 mgR
N
Alveolar chord (μm)
120
100
80
60
40
20
0
*
*
*
Emilin1 +/+ -/- +/+ -/-
Fibrillin-1 +/+ +/+ mgR mgR

supports our model on the genetic and functional link between Emilin1 and TGF-β. Moreover, the similarity of the lung phenotype constituted an ideal setting for testing the epistatic relationship between Emilin1 and Fibrillin-1. If Emilin1 acted through Fibrillin, one should expect that loss of Emilin1 had no major effects on the Fibrillin mutant phenotype. On the contrary, the results showed that simultaneous mutation of the two genes greatly aggravated the alveolar phenotype (Figures 4M and 4N), favoring the idea that Emilin1 and Fibrillin act primarily through independent/parallel pathways to regulate TGF-β signaling. This is also supported by the histological analysis of the fine morphology and dimensions of elastic lamellae of aortas explanted from double knockout mice as well as of mice survival kinetics (Figures S5E– S5K).

DISCUSSION

Emilin1 Is a proTGF-β Antagonist

This paper has identified a new mechanism of regulation of arterial blood pressure based on the function of the elastic fiber glycoprotein Emilin1 as modulator of TGF-β signaling (Figure 5).

Using *Xenopus* embryos and human cells as read-outs of TGF-β activity, we established a role for Emilin1 as antagonist of TGF-β signals. We found that Emilin1 overexpression is unable to contrast the activity of mature TGF-β1 but is effective against the immature proTGF-β. Moreover, by using cells derived from the Emilin1 knockout mice, we showed that, at the physiological level, Emilin1 is required to dampen TGF-β activity. This biological property parallels with the specific physical interaction of Emilin1 with proTGF-β. This represents a novelty in the mechanisms of action of secreted antagonists of growth factors, such as Chordin or Cerberus/Dan, as these molecules antagonize mature, fully processed ligands and compete with their cognate receptors (Piccolo et al., 1999).

Mechanism of Emilin1 Activity

We have presented evidences indicating that Emilin1 prevents the processing of proTGF-β into LAP and mature TGF-β, a key event for TGF-β availability. Overexpression of Emilin1 promotes the accumulation of unprocessed proTGF-β at the expense of mature TGF-β; oppositely, proTGF-β1 is readily cleaved in *Emilin1* mutant cells, and its stability can be rescued upon blockade of furin proteases (Figure 3H).

Finding a new tier of regulation at the level of TGF-β maturation was interesting, as previous studies focused primarily on downstream events, including proper localization of the latent LAP/TGF-β complex within the extracellular milieu (Koli et al., 2004), and on factors exposing mature TGF-β to its receptors (Figure 5). In contrast, the study of the very initial steps controlling TGF-β bioavailability, such as secretion and processing, received much less attention, likely due to the lack of specific genes or animal models for molecules controlling these processes. The identification of Emilin1 and the generation of Emilin1 mutant animals represent a step forward in this field.

Our data suggest that Emilin1 prevents proTGF-β processing in the extracellular space, as expected for an ECM molecule. First, artificial retention of Emilin1 within the secretory pathway does not inhibit TGF-β activity (Figure 3N), suggesting that Emilin1 must operate in the extracellular compartment to act as antagonist. Second, by mixing distinct cell populations, we found that Emilin1 is required and sufficient to counteract TGF-β even when present only in cells receiving the signal (Figures 3L and 3M). These data are in line with reports from Constam and coworkers, who showed that SPC/furin proteases are required extracellularly to process TGF-β and must act non-cell-autonomously during embryonic development (Beck et al., 2002).

In Vivo Requirements of Emilin1 as TGF-β Antagonist for Blood Pressure Control

In addition to in vitro studies, we validated in vivo the relevance of *Emilin1* as TGF-β antagonist by examining cells and tissues from Emilin1 knockout mice. A great deal of evidence supports our conclusion, at least in the vascular

Figure 4. Increased TGF-β Activity Is Required for the Development of the Emilin1 Phenotype

(A and B) Increased TGF-β signaling in Emilin1-deficient aorta as revealed by anti-P-Smad2 immunoperoxidase staining of ascending aorta. Age of mice: 2 months. Bar = 25 μm.

(C) Quantitative evaluation of the increase of the number of P-Smad2 positive nuclei in mutant mice. Values are mean ± SD. *$p < 0.01$ versus wild-type.

(D and E) Increased TGF-β signaling in Emilin1-deficient aorta as revealed by expression of the *CAGA12/GFP* transgene. The *CAGA2/GFP* transgene was developed into *Emilin1*$^{+/+}$ and *Emilin1*$^{-/-}$ backgrounds, and corresponding sections from ascending aortas were stained in parallel with an antibody against GFP using the immunoperoxidase procedure. Age of mice: 2 months. Bar = 25 μm.

(F) Activation of the TGF-β target gene PAI-1 in Emilin1-deficient aorta revealed by Western blotting. +/+ wild-type animal; −/− *Emilin1* mutant animal. Age of mice: 8 months.

(G and H) Dependence of the Emilin1 phenotype from *TGF-β1* gene dosage. Mice with the indicated genotypes were generated by crossing *Emilin1*$^{+/-}$ and *TGF-β1*$^{+/-}$ double heterozygous animals. (G) Systolic blood pressure evaluated noninvasively by tail-cuff plethysmography in conscious mice (n = 6 for each genotype). *$p < 0.01$ versus *Emilin1*$^{+/+}$;*TGFβ1*$^{+/+}$ mice. (H) Media cross-sectional area (MCSA) of mesenteric arteries evaluated using a Mulvany myograph (n = 5 for each genotype). *$p < 0.01$ versus *Emilin1*$^{+/+}$;*TGFβ1*$^{+/+}$. Data are mean ± sem.

(I) Representative echocardiographic analysis of ascending aorta in offspring from *Emilin1*$^{+/-}$ and *TGF-β1*$^{+/-}$ crossings (n = 4 for each genotype).

(J–M) Histological sections of lung from mice generated from *Emilin1* and *Fibrillin-1* double heterozygous crosses. *Emilin1* (K) and *Fibrillin-1* (L) mutant mice (−/− and *mgR,* respectively) show enlarged alveolar spaces. mgR mutation is a severe hypomorphic *Fibrillin-1* allele, which was always used here in homozygosity (*mgR/mgR*). The alteration is further increased in double homozygous mutants (M). Bar = 50 μm.

(N) Quantitative evaluation of the effect described in (J–M). *$p < 0.001$ versus wild-type.

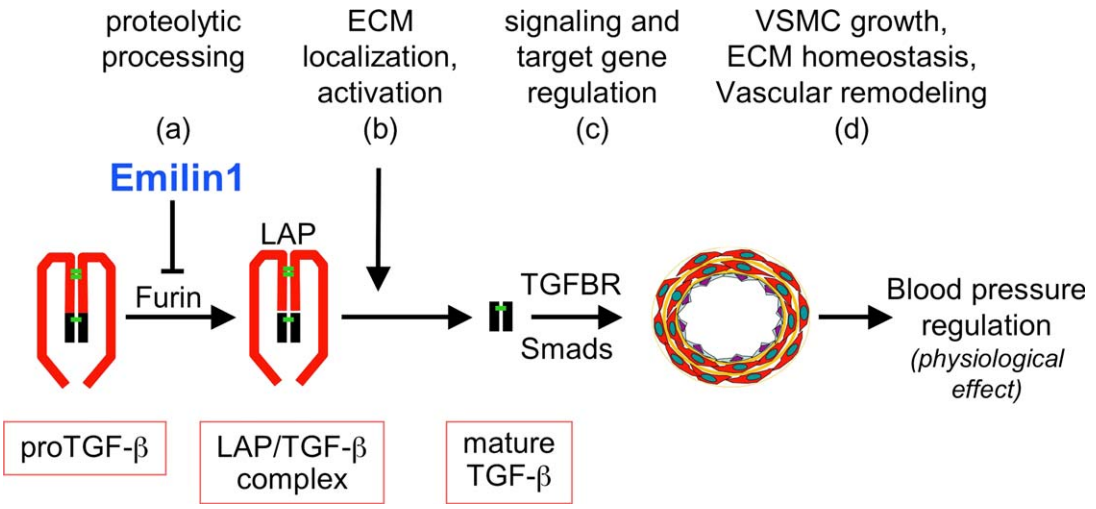

Figure 5. Model of Emilin1 Activity as Antagonist of TGF-β Signaling in the Vascular Wall

(A) The TGF-β precursor (proTGF-β) is cleaved by proprotein convertases, giving rise to the formation of the LAP-TGF-β complex; Emilin1 inhibits this processing step. On its turn, the LAP-TGF-β complex (or small latent complex) becomes localized and specifically targeted to the extracellular milieu by LTBP proteins (B). LTBPs are also required for TGF-β activation, namely, the retrieval of free mature TGF-β from the LAP (Koli et al., 2004). TGF-β activation is also stimulated by αvβ6 integrin and other ECM molecules, such as Thrombospondin-1 (Annes et al., 2003). Signaling through the TGF-β receptor (TGFBR) results in changes of gene expression (C), with consequences on vascular SMC growth and phenotype, ECM homeostasis, and vascular remodeling (D).

system. First, the level of P-Smad2 staining increased in Emilin1 mutant aortas when compared to the wild-type tissue (Figure 4C), as expected from the loss of a TGF-β inhibitor. Second, transcription from a transgenic TGF-β reporter was enhanced in the Emilin1 mutant background. Third, the endogenous levels of TGF-β target genes, such as PAI-1 and c-Myc, are dysregulated in vascular explants from Emilin1 mutants. Further, we found an abnormal increase of alveolar airspace in Emilin1 mutants, a developmental defect previously linked to excess of TGF-β signaling (Neptune et al., 2003).

Our data support the notion that the antagonism to TGF-β is crucial to explain hypertension in Emilin1 deficient animals. Indeed, we found that lowering back TGF-β levels is sufficient to rescue the vascular defects and the blood pressure to normal levels. Whether defects in Emilin1 underlie some forms of human hypertension remains to be investigated; yet our study unveils the importance of considering mechanisms affecting TGF-β signaling to shed light on this human disease. Of note, variations in the TGF-β signal peptide that may enhance the production of the cytokine have been already correlated to increased risk of hypertension in humans (Suthanthiran et al., 2000). In Emilin1 mutants, hypertension is likely caused by developmental perturbation on vessel size; nevertheless, this perturbation might predispose to a late-onset, seemingly acquired disease, bringing about an increased peripheral resistance. Intriguingly, studies in the spontaneous hypertensive rat model revealed that the hypertension has its incipit in the reduced lumen of the resistance vasculature; still, the hypertensive phenotype is not manifest in young animals (Mulvany, 2002). These remain largely unexplored fields.

We think that a relevant cause of the Emilin1 phenotype is the reduced vascular growth due to excess of TGF-β signaling. Accordingly, we found reduced proliferation capacity of primary SMC isolated from mutant vessels. This result parallels with the level of c-Myc, a TGF-β repressed target and key mediator of SMC proliferation (Khanna, 2004): c-Myc levels are reduced in mutant aortas but rescued in the compound *Emilin*$^{-/-}$*;TGF-β*$^{+/-}$ genetic setup. That said, TGF-β is a potent cytokine with multiple target genes; therefore, its dysregulation might trigger pleiotropic effects, including changes in growth factor responsiveness, cellular fate, differentiation, tissue renewal, and others. For instance, we did document in Emilin1 mutant aortas a mild fibrosis (increased collagen I deposition) a well-known effect of persistent TGF-β activity (Figure S6).

The Emilin1 Mutant Phenotype

Elastic fibers are made of two distinct morphological components, an amorphous core, composed mainly by the fibrous protein Elastin, and a coat of microfibrils, whose major constituent is Fibrillin-1, the gene affected in patients with Marfan syndrome (Dietz et al., 1991). Since Fibrillin-1 has been shown to be a negative regulator of TGF-β activity in some tissues (Neptune et al., 2003), an aspect that deserves discussion is the comparison between the Emilin1 and the Fibrillin-1 phenotype. In principle, the possibility existed that the Emilin1 defects might be secondary to compromised Fibrillin-1 function. However, our data do not favor this possibility: Not only was the Fibrillin-1 network normal in Emilin1-deficient tissues, but we found no evidence of an epistatic relationship between Emilin1

and Fibrillin-1. Indeed, the simultaneous mutation of the two genes concurred in aggravating their similar lung phenotype, and the aortic defects in double knockout mice were a combination of those found in single mutants (Figure 4). Thus, Emilin1 and Fibrillin-1 may regulate TGF-β either through qualitatively different mechanisms or by acting at different developmental stages. One possibility is that Emilin1 might be primarily required during early vessel morphogenesis, and its absence might impose a bias on vascular cell growth, leading to hypoplasia and hypertension; the prominent role of Fibrillin-1 in elastic matrix and vascular wall homeostasis would emerge and dominate at later stages.

Considering the extent of regulation caused by Emilin1 in cultured MEFs and aortas, the phenotype of Emilin1 might appear surprisingly mild. Yet several mechanisms might intervene to attenuate and balance the effects of Emilin1 in the whole organism. First, the Emilin family enlists seven proteins, allowing for a high complexity of regulation of TGF-β signaling by EMI-domains: Redundancy between family members might compensate for Emilin1 inactivation. Second, one has to consider that the expression pattern of Emilin1 and of its relative TGF-β ligands should closely overlap in order for the two molecules to control a phenotypic trait. For instance, although Nodal is blocked by Emilin1 in heterologous assays, Emilin1 and its family members are not coexpressed with Nodal in early embryos: Thus, *Emilin1* knockouts develop normally, without mesodermal expansion. Conversely, *TGF-β1* is essential for development and homeostasis of the vascular system (Agrotis et al., 2005); in line, the sole TGF-β1 haploinsufficiency is sufficient to rescue the vascular phenotype of Emilin1 mutants. Third, while processing of proTGF-β1 appears as an essential step for TGF-β availability in the cells and tissues here investigated, in other contexts downstream extracellular events may become rate-limiting, including the mobilization of the latent TGF-β from the extracellular matrix or its activation prior to receptor binding (Figure 5). Finally, a further level of complexity is the presence of feedback loops between TGF-β family members, BMPs, and their extracellular regulators: This would lead to a fine-tuning of signaling and to the appearance of context- or tissue-restricted phenotypes (Koli et al., 2004).

The discovery of Emilin1 as regulator of TGF-β processing and activation may be relevant not only for hypertension but also for many other pathological conditions in which TGF-β has been suggested to play a role, such as atherosclerosis, inflammation, tissue repair, fibrosis, and cancer.

EXPERIMENTAL PROCEDURES

Transgenic Mice

Generation of mice with one inactivated *Emilin1* allele was as previously described (Zanetti et al., 2004).

Mice carrying a null mutation in the *TGF-β1* gene on a mixed SvEv129 × C57BL/6 background were kindly provided by Dr. A.B. Roberts (National Cancer Institute, National Institutes of Health, Bethesda, MD, USA). These mice were mated with *Emilin1*$^{-/-}$ mice derived from C57BL/6NCrlBR backcrosses. *Emilin1*$^{-/-}$ and *Emilin1*$^{+/+}$ mice harboring a reporter gene sensitive to TGF-β signaling were generated by appropriate breeding of the *Emilin1*$^{-/-}$ animals with the *CAGA12/GFP* transgenic strain (obtained from Dr. H.C. Dietz).

Mice with the *mgR* hypomorphic mutation of the *Fibrillin-1* gene were provided by Dr. F. Ramirez.

Evaluation of Blood Pressure, Echocardiographic Analysis, and Vessel Extensibility

Blood pressure was evaluated noninvasively by tail-cuff plethysmography. For radiotelemetric analysis, the left femoral artery of anaesthetized mice was exposed and cannulated with a 0.4 mm catheter connected to a radiotelemetric device (TA11PA-C20, Data Sciences International) anchored subcutaneously. After recovery (7 days), blood pressure and heart rate were monitored continuously six times a day for 20 days. Mean value was calculated with the software DQ ART 1.1 Gold (Data Sciences International).

Echocardiographic analysis was performed as previously described (De Acetis et al., 2005) using either a 7.5 MHz or a 30 MHz imaging transducer. For vessel extensibility evaluation, carotid artery was placed in a pressure myograph on an inverted microscope connected to a charge-coupled device camera and a computer system, allowing continuous measurement of internal and external diameter. Intravascular pressure was increased stepwise from 20 to 200 mmHg. Extensibility was calculated using the following formula: extensibility at a defined pressure ($\underline{p}$) = ([diameter at $\underline{p}$ + 25 mmHg − diameter at $\underline{p}$ − 25 mmHg] / [diameter at $\underline{p}$ − 25 mmHg]) × 100.

Plasmids

For the complete list of plasmids, please refer to Supplemental Data.

Biological Assays in *Xenopus*

Xenopus embryos manipulations, capped mRNA preparations, and whole-mount in situ hybridizations were performed as previously described (Piccolo et al., 1999). For RT-PCR, conditions and primers were as described in http://www.hhmi.ucla.edu/derobertis/.

Cell Culture and Transfection

For luciferase assays, HEK293T cells were transfected with the indicated plasmids using Lipofectamine2000 (Invitrogen); embryonic fibroblasts (MEFs) from wild-type and knockout *Emilin1* mice were transfected using LipofectAMINE PLUS (Invitrogen). pCMV-lacZ was used to normalize for transfection efficiency.

For experiments in Figures 3I and 3K, cells were incubated with 100 μM decanoyl-RVKR-chloromethylketone (Alexis), adding the compound every 12 hr, whereas controls were treated with carrier alone.

For experiments shown in Figure 3C, MEFs cells were incubated with 5 μM SB431542 (Tocris) for 48 hr in DMEM supplemented with 2% FBS. For experiments in Figures 3D and 3M, MEFs cells were incubated with 20 μM SP600125 (Calbiochem) for 48 hr in DMEM supplemented with 2% FBS. For cell-mixing experiments, Responding and Stimulator cell populations were trypsinized and mixed together and replated (for Stimulator MEFs in Figure 3M, after mixing, cells were cultured in media without drug). After 36 hr starvation in DMEM supplemented with 0.1% FBS (HEK293T cells) or after 18 hr starvation in DMEM supplemented with 2% FBS (MEFs), cells were harvested for luciferase assay. Every sample was transfected in triplicate, and every experiment was repeated at least two times.

Immunoprecipitation and Protein Blotting

HEK293T cells were transfected with the calcium-phosphate method. Cells were harvested in ice-cold 25 mM Tris pH 7.5, 150 mM NaCl, 2.5 mM EDTA, 10% Glycerol, 1% NP40, protease inhibitors (Roche); NP40 was diluted to 0.1% for IP. Where indicated, 150 ng purified recombinant LAP (R&D) was added to lysates prior to IP (Piccolo et al., 1999). For Western blotting, protein samples were resolved under reducing or

nonreducing (Figure 3E only) conditions by SDS-PAGE and blotted onto PVDF membranes. Please refer to Supplemental Data for details on the immunodetection procedure.

Supplemental Data

Supplemental Data include six figures, one table, Experimental Procedures, and References and can be found with this article online at http://www.cell.com/cgi/content/full/124/5/929/DC1/.

ACKNOWLEDGMENTS

We thank D. Forrest for the gift of antiserum against mouse Emilin1; A.B. Roberts for providing mice with an inactivating mutation in the *TGF-β1* gene; H.C. Dietz for the *CAGA12/GFP* transgenic mouse line; F. Ramirez for the *Fibrillin-1 mgR* mutant mice. This work was supported by grants from Comitato Promotore Telethon, AIRC, and ISS to S.P.; from MIUR-FIRB to S.P. and G.M.B.; and from MIUR-PRIN to S.P., D.V., G.L., and G.M.B.

Received: July 19, 2005
Revised: November 18, 2005
Accepted: December 14, 2005
Published: March 9, 2006

REFERENCES

Agrotis, A., Kalinina, N., and Bobik, A. (2005). Transforming growth factor-beta, cell signaling and cardiovascular disorders. Curr Vasc Pharmacol *3*, 55–61.

Annes, J.P., Munger, J.S., and Rifkin, D.B. (2003). Making sense of latent TGFbeta activation. J. Cell Sci. *116*, 217–224.

Beck, S., Le Good, J.A., Guzman, M., Ben Haim, N., Roy, K., Beermann, F., and Constam, D.B. (2002). Extraembryonic proteases regulate Nodal signalling during gastrulation. Nat. Cell Biol. *4*, 981–985.

Braghetta, P., Ferrari, A., De Gemmis, P., Zanetti, M., Volpin, D., Bonaldo, P., and Bressan, G.M. (2004). Overlapping, complementary and site-specific expression pattern of genes of the EMILIN/Multimerin family. Matrix Biol. *22*, 549–556.

Bressan, G.M., Daga-Gordini, D., Colombatti, A., Castellani, I., Marigo, V., and Volpin, D. (1993). Emilin, a component of elastic fibers preferentially located at the elastin-microfibrils interface. J. Cell Biol. *121*, 201–212.

De Acetis, M., Notte, A., Accornero, F., Selvetella, G., Brancaccio, M., Vecchione, C., Sbroggio, M., Collino, F., Pacchioni, B., Lanfranchi, G., et al. (2005). Cardiac overexpression of melusin protects from dilated cardiomyopathy due to long-standing pressure overload. Circ. Res. *96*, 1087–1094.

Dietz, H.C., Cutting, G.R., Pyeritz, R.E., Maslen, C.L., Sakai, L.Y., Corson, G.M., Puffenberger, E.G., Hamosh, A., Nanthakumar, E.J., Curristin, S.M., et al. (1991). Marfan syndrome caused by a recurrent de novo missense mutation in the fibrillin gene. Nature *352*, 337–339.

Eimon, P.M., and Harland, R.M. (2002). Effects of heterodimerization and proteolytic processing on Derriere and Nodal activity: implications for mesoderm induction in Xenopus. Development *129*, 3089–3103.

Faury, G., Pezet, M., Knutsen, R.H., Boyle, W.A., Heximer, S.P., McLean, S.E., Minkes, R.K., Blumer, K.J., Kovacs, A., Kelly, D.P., et al. (2003). Developmental adaptation of the mouse cardiovascular system to elastin haploinsufficiency. J. Clin. Invest. *112*, 1419–1428.

Inman, G.J., Nicolas, F.J., Callahan, J.F., Harling, J.D., Gaster, L.M., Reith, A.D., Laping, N.J., and Hill, C.S. (2002). SB-431542 is a potent and specific inhibitor of transforming growth factor-beta superfamily type I activin receptor-like kinase (ALK) receptors ALK4, ALK5, and ALK7. Mol. Pharmacol. *62*, 65–74.

Izzo, J.L., Jr., and Shykoff, B.E. (2001). Arterial stiffness: clinical relevance, measurement, and treatment. Rev. Cardiovasc. Med. *2*, 29–34, 37–40.

Khanna, A. (2004). Concerted effect of transforming growth factor-beta, cyclin inhibitor p21, and c-myc on smooth muscle cell proliferation. Am. J. Physiol. Heart Circ. Physiol. *286*, H1133–H1140.

Koli, K., Wempe, F., Sterner-Kock, A., Kantola, A., Komor, M., Hofmann, W.K., von Melchner, H., and Keski-Oja, J. (2004). Disruption of LTBP-4 function reduces TGF-beta activation and enhances BMP-4 signaling in the lung. J. Cell Biol. *167*, 123–133.

Mongiat, M., Mungiguerra, G., Bot, S., Mucignat, M.T., Giacomello, E., Doliana, R., and Colombatti, A. (2000). Self-assembly and supramolecular organization of EMILIN. J. Biol. Chem. *275*, 25471–25480.

Mulvany, M.J. (2002). Small artery remodeling and significance in the development of hypertension. News Physiol. Sci. *17*, 105–109.

Neptune, E.R., Frischmeyer, P.A., Arking, D.E., Myers, L., Bunton, T.E., Gayraud, B., Ramirez, F., Sakai, L.Y., and Dietz, H.C. (2003). Dysregulation of TGF-beta activation contributes to pathogenesis in Marfan syndrome. Nat. Genet. *33*, 407–411.

Piccolo, S., Agius, E., Leyns, L., Bhattacharyya, S., Grunz, H., Bouwmeester, T., and De Robertis, E.M. (1999). The head inducer Cerberus is a multifunctional antagonist of Nodal, BMP and Wnt signals. Nature *397*, 707–710.

Siegel, P.M., and Massague, J. (2003). Cytostatic and apoptotic actions of TGF-beta in homeostasis and cancer. Nat. Rev. Cancer *3*, 807–821.

Staessen, J.A., Wang, J., Bianchi, G., and Birkenhager, W.H. (2003). Essential hypertension. Lancet *361*, 1629–1641.

Suthanthiran, M., Li, B., Song, J.O., Ding, R., Sharma, V.K., Schwartz, J.E., and August, P. (2000). Transforming growth factor-beta 1 hyperexpression in African-American hypertensives: A novel mediator of hypertension and/or target organ damage. Proc. Natl. Acad. Sci. USA *97*, 3479–3484.

Ventura, J.J., Kennedy, N.J., Flavell, R.A., and Davis, R.J. (2004). JNK regulates autocrine expression of TGF-beta1. Mol. Cell *15*, 269–278.

Zanetti, M., Braghetta, P., Sabatelli, P., Mura, I., Doliana, R., Colombatti, A., Volpin, D., Bonaldo, P., and Bressan, G.M. (2004). EMILIN-1 deficiency induces elastogenesis and vascular cell defects. Mol. Cell. Biol. *24*, 638–650.